

Definition of the Polar Vortex Edge by LIDAR Data of the Stratospheric Aerosol: A Comparison with Values of Potential Vorticity

by M. DAMERIS, M. WIRTH, W. RENGER and V. GREWE

Institut für Physik der Atmosphäre, DLR Oberpfaffenhofen, D-82230 Weßling, Germany

(Manuscript received November 30, 1994; accepted January 31, 1995)

Abstract

In this paper LIDAR data of stratospheric aerosol measured during four long range flights (during Northern Hemisphere winter) by the German research aircraft TRANSALL are employed to describe the edge of the polar vortex. All flights directly crossed the polar vortex edge. The position of the boundary of the vortex is clearly identified in the data. Values of potential vorticity on isentropic surfaces often used to describe the structure and edge of the polar vortex are calculated as well. They are interpreted with respect to the aerosol data. A comparison with previously published diagnostics of the edges of the polar vortices shows good agreement.

Zusammenfassung

Bestimmung des Randes des Polarwirbels mittels LIDAR-Beobachtungen von stratosphärischem Aerosol: Ein Vergleich mit Werten der potentiellen Vorticity

In dieser Arbeit werden Messungen von stratosphärischem Aerosol benutzt um den Rand des polaren Stratosphärenwirbels zu beschreiben. Während vierer Langstreckenflüge mit dem deutschen Forschungsflugzeug TRANSALL wurden die Messungen mit einem Aerosol und Ozon LIDAR durchgeführt. Alle Flüge führten direkt durch den Rand des Polarwirbels. Die Lage des Wirbelrandes kann in den Daten eindeutig identifiziert werden. Zusätzlich werden Werte der potentiellen Vorticity auf isentropen Flächen berechnet. Diese werden häufig benutzt um die Struktur und den Rand des Wirbels zu beschreiben. Die berechneten Werte der potentiellen Vorticity werden mit den Aerosoldaten gemeinsam interpretiert. Bereits früher veröffentlichte Daten zur Beschreibung des Wirbelrandes werden verglichen, sie zeigen eine gute Übereinstimmung.

1 Introduction

In the Northern Hemisphere it is difficult to separate the contribution of dynamical and chemical processes to the development of low ozone values. In contrast to the Southern Hemisphere, highly variable dynamical processes (e.g. planetary wave activity) play an important role for the ozone distribution. A clear indication of the differences between the hemispheres is the characteristic behaviour of the polar vortex during winter, which is significantly more variable in the Northern Hemisphere. The dynamics of the winter stratospheric polar vortex play a key role for the ozone distribution. The knowledge of the degree of the isolation of

air within the vortex is important for the interpretation of chemical data. Recently, several papers dealing with problems of air mass exchange between the polar vortex and its environment have been published (e.g. Chen, 1994; Chen et al., 1994; Waugh et al., 1994; Günther and Dameris, 1995). The analysis of possible exchange processes across the vortex edge presumes the knowledge of the structure of the polar vortex with respect to its vertical and horizontal shape, in particular the position of the vortex boundary.

The edge of the polar vortex has been determined earlier by several authors. One general impression is that the "edge" of the polar vortex is a narrow transition zone and cannot be adequately defined by

a single value of any parameter. In the following, only some of the recently published data are mentioned.

For example, Manney and Zurek (1993) used contours of potential vorticity (PV) to describe the vortex boundary. These contours have been determined near the equatorward side of the region of strong gradients of PV that tend to isolate the polar vortex. Rummukainen et al. (1994) did a quantitative comparison of wind-maxima and isentropic PV diagnostics of the polar vortices in the Arctic (1992 and 1993) and in the Antarctic (1992). They found that both the maximum wind speed and discrete PV-ranges seem to be acceptable parameters for describing the edge of the polar vortex. Manney et al. (1994a) presented vertical sections of scaled PV (see Section 3) for late February and early March 1993 compared with N₂O-data (measured by the Cryogenic Limb Array Etalon Spectrometer (CLAES) on board the Upper Atmosphere Research Satellite (UARS)). The results indicate that the vortex edge during this time period might reasonably be defined by particular values of scaled PV.

There are clear indications (e.g. Manney et al., 1994b and 1994c; besides the above mentioned papers) that the values of PV used to determine the position of the vortex edge varies considerably with time of winter, hemisphere, height and also from year to year.

The investigation of concentration profiles of atmospheric tracers (e.g. N₂O, CH₄) near the vortex edge is one possibility to determine and to describe the edge of the polar vortex (see above). For this paper, LIDAR-aerosol data of four flights (January 27, 1993; March 10, 1993; February 15, 1994; March 16, 1994) measured during long range missions with the German research aircraft TRANSALL have been used. At this time, the atmosphere still contained enough Pinatubo aerosol to distinguish different stratospheric air masses by their aerosol content, especially at the edge of the polar vortex. All flights directly crossed the vortex edge. The aerosol data show that in each case the vortex interior is characterized by low aerosol concentrations indicating stronger descent of "aerosol free" air from the upper stratosphere within the vortex. Manney et al. (1994b) analysed trajectory calculations for the years 1992 to 1994 in the Southern and Northern Hemisphere. They pointed out that in early winter, the Northern Hemisphere shows strongest descent near the center of the vortex, except when wave activity is particularly strong. In late winter, parcels descent less and the polar night jet

moves downward. Nevertheless, the amount and patterns of descent remain subject of considerable debate (e.g. Randel, 1993).

Measurements of stratospheric aerosols offer an additional possibility to describe the structure of the polar vortex, especially of its edge. The aerosol measurements can be compared with other measurements (e.g. of wind speed or tracers like N₂O) and theoretical approaches (calculation of PV).

For the present investigation, ECMWF analyses on pressure levels (12 GMT, resolution 2.5° × 2.5°) are used to calculate potential vorticity values on isentropic surfaces. The meteorological analyses for the dates of flights, used to calculate PV, have been provided by NILU (Norwegian Institute for Air Research) for members of the TRANSALL campaigns which have been part of European campaigns (e.g. SESAME – Second European Stratospheric and Midlatitude Experiment).

The following section briefly describes the principles of the aerosol measurements and the data evaluation. In Section 3, results of the aerosol measurements are presented. Based on these data, the position of the "edge" of the polar vortex has been determined. Related values of potential vorticity on isentropic surfaces are calculated with a short comparison with earlier published results. A conclusion follows in Section 4.

2 Experimental Setup and Data Evaluation

For the purpose of studying the dynamics of stratospheric ozone, a combined aerosol and ozone LIDAR, named OLEX (Ozone Lidar Experiment) has been developed at DLR (e.g. Wirth et al., 1994). It is an airborne instrument that permits the recording of two-dimensional backscatter profiles at three different wavelengths (532 nm, 354 nm, 308 nm). From these profiles, it is possible to calculate the spatial distribution, backscatter ratios and (assuming an aerosol model) extinction coefficients of stratospheric aerosols and clouds. In this paper, only results of the aerosol part (the 532 nm channel) are used.

The total backscatter ratio used for this investigation is defined by β/β_R where $\beta = \beta_M + \beta_R$ (sum of particle- and molecular backscattering) and β_R is the molecular backscatter coefficient of air. The backscatter ratio can be interpreted as particle mixing ratio (ratio between backscatter coefficient of particles with respect to clean air). This quantity is approximately conserved following an air parcel.

Backscatter Ratio at 532nm on 27. Jan. 93
with Contours of Potential Vorticity

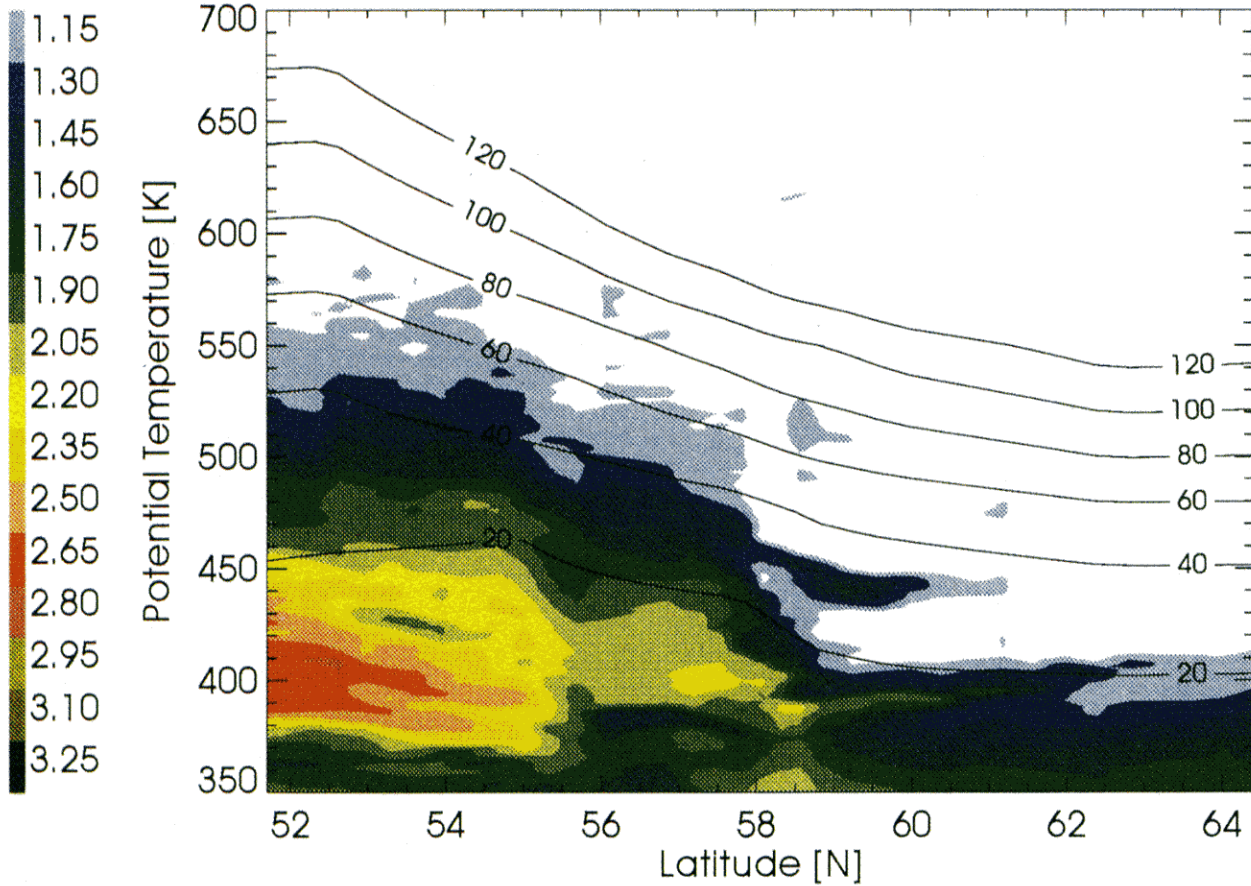


Figure 1a Contour plot of the backscatter ratio at 532 nm with contours of potential vorticity for the TRANSALL flight on 27. January 1993.

Backscatter Ratio at 532nm on 28. Jan. 94
with Contours of Potential Vorticity

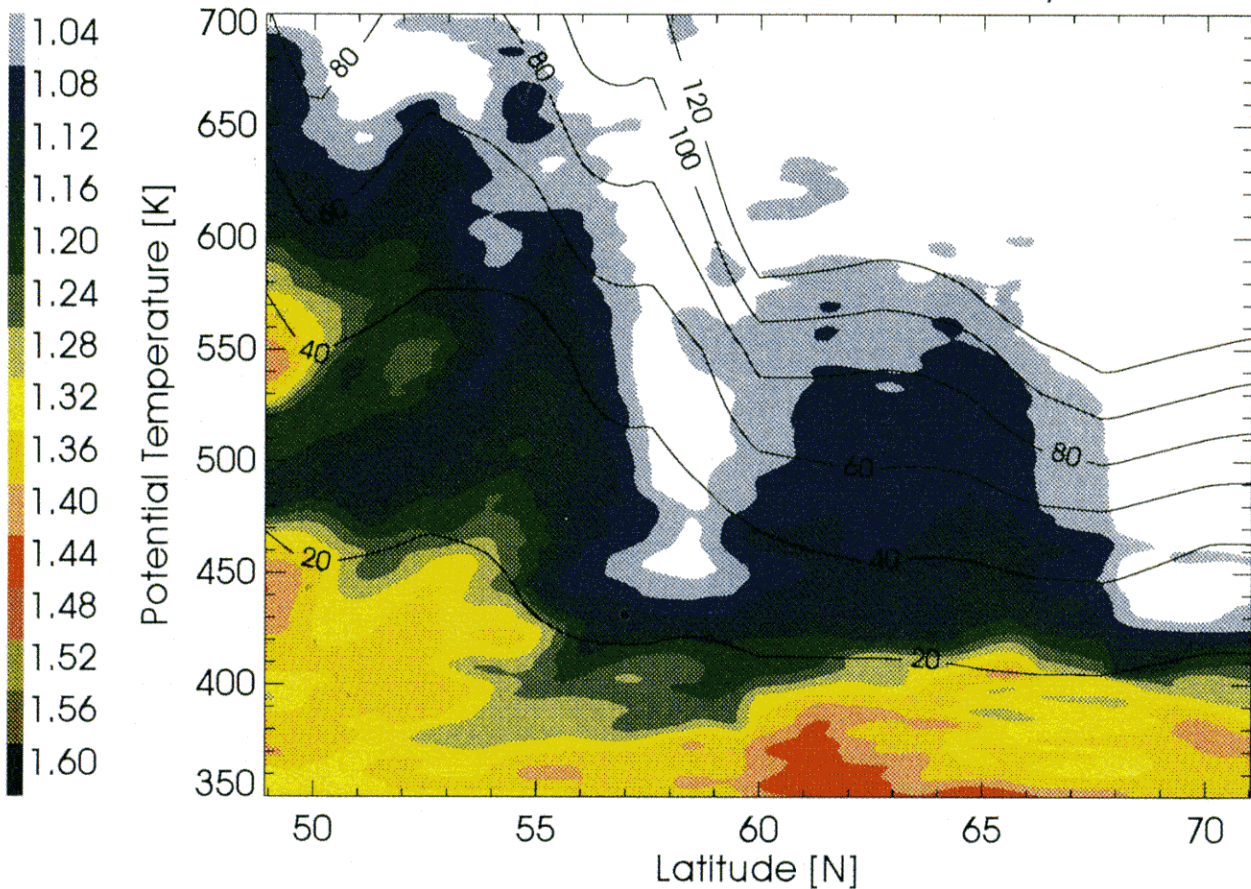


Figure 1b As Figure 1a, but on 28. January 1994.

Table 1 Values of potential vorticity evaluated on isentropic surfaces at positions where the backscatter ratio decreased to 70 %, 50 %, and 30 %, respectively, with regards to a 100 % value describing the situation outside the vortex. Units are $10^{-6} \text{ K m}^2 \text{ kg}^{-1} \text{ s}^{-1}$

date	%	PV		
		435 K	475 K	550 K
	70	18.3	24.6	64.4
27.01.1993	50	19.9	30.3	67.6
	30	22.1	33.6	85.6
	70	24.0	30.5	51.3
10.03.1993	50	23.5	30.4	54.3
	30	19.8	30.1	58.1
	70	16.2	22.9	40.3
15.02.1994	50	16.3	26.3	40.6
	30	16.4	28.7	41.1
	70	22.2	35.7	58.1
16.03.1994	50	26.3	36.1	70.2
	30	29.1	37.2	74.6
mean	50	21.5	30.8	58.2

For the calculation of the backscatter ratio 1000 laser shots have been averaged, resulting in a horizontal resolution of approximately 25 km (depending on the speed of the aircraft). Data are available for the height range from 10 to 28 km with a resolution of 60 m. A standard correction method for the aerosol extinction was applied which assumes a particle size distribution and a value for the refractive index of the aerosol droplets (Deshler, 1994).

A more detailed description of the OLEX system, the applied corrections, and the evaluation of the data was given by Wirth et al. (1994).

3 Comparison of Aerosol Data and Potential Vorticity

Measurements of four flights have been chosen for this investigation. Figure 1a shows the distribution of the backscatter ratio at 532 nm along the flight path on January 27, 1993, including contours of potential vorticity. It is obvious that the aerosol data (backscatter ratio) show strong gradients in the vicinity of the edge of the polar vortex, indicating

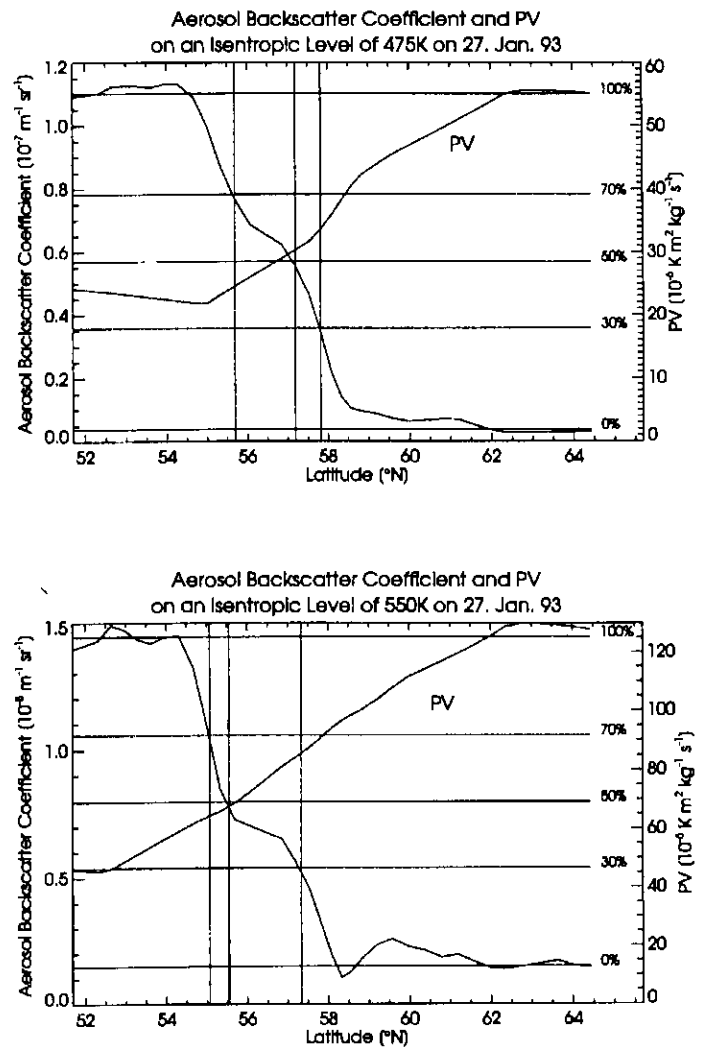


Figure 2 Contour plot of the aerosol backscatter coefficient and potential vorticity on isentropic level 475 K (a) and 550 K (b) along the flight path on 27. January 1993. The vertical and horizontal lines indicate where the aerosol backscatter coefficient decreased to 70 %, 50 %, and 30 %, respectively (see text).

reduced mixing. Similar figures have been found for the other flights (not shown). Figures 2 to 5 show the backscatter ratio for the 475 K (a) and the 550 K (b) isentropic surfaces along the flight path for January 27, 1993, March 10, 1993, February 15, 1994, and March 16, 1994. The vertical lines in Figures 2 to 5 indicate at which latitude (longitude) the backscatter ratio decreased to 70 %, 50 %, and 30 %, respectively, with regards to a backscatter ratio value describing the situation outside the vortex (100 % value). The interval between the 70 %- and the 30 %-values describes approximately the transition zone dividing air masses inside and outside the polar vortex (i.e., the vortex "edge"). Additionally, Figures 2 to 5 give the corresponding

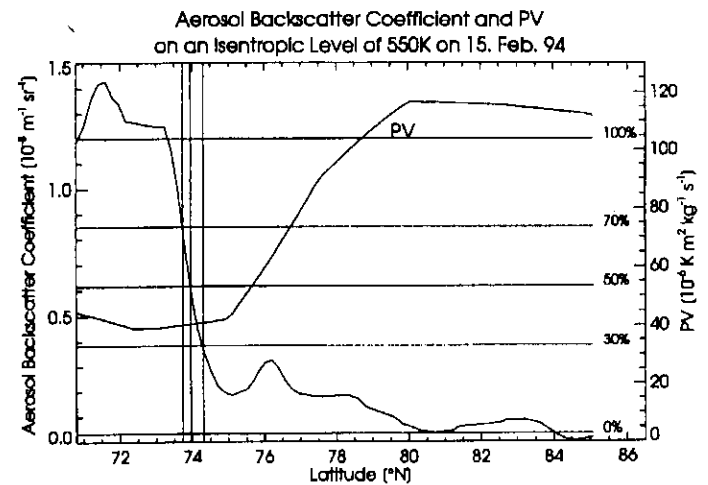
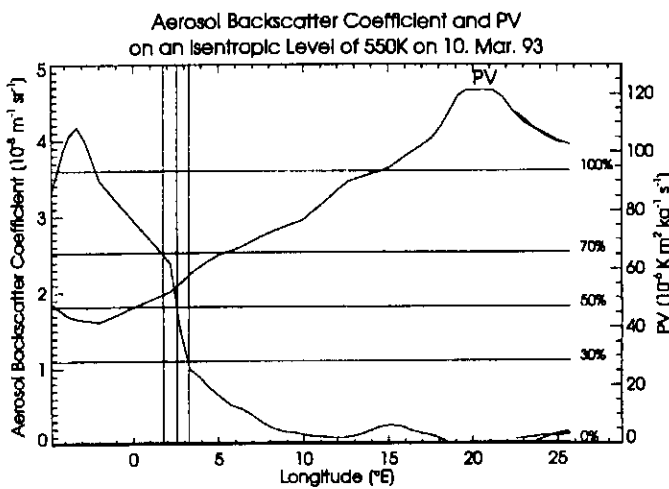
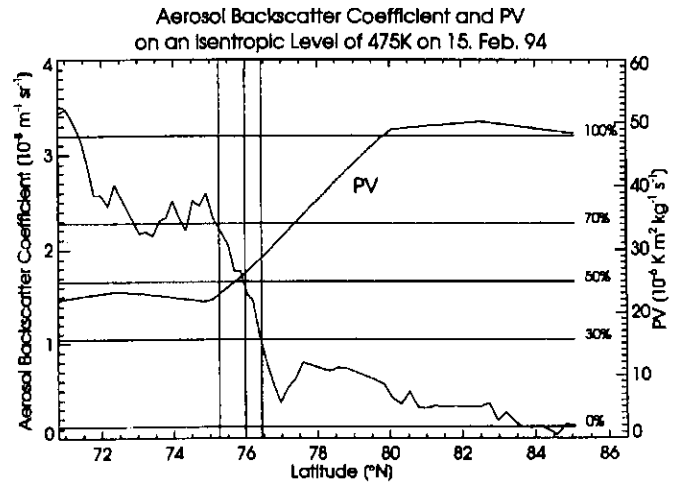
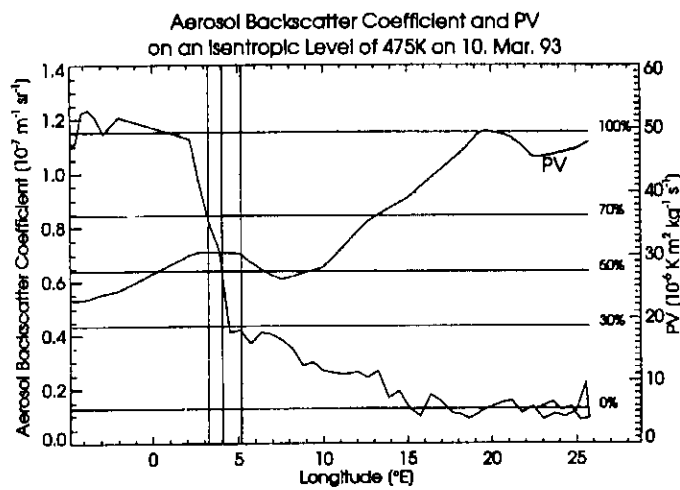


Figure 3 As Figure 2, but on 10. March 1993.

Figure 4 As Figure 2, but on 15. February 1994.

values of potential vorticity along the flight paths. The meteorological analyses used for the calculations of PV are available for 12 GMT. The measurements of the aerosol data were made between 9.30 and 11 GMT, except on March 16, 1994, where the measurement period lasted between 18.30 and 19.30 GMT. In particular, for the first three flights the discrepancy in time should not affect significantly the comparison of aerosol data and PV. Following McIntyre and Palmer (1983), the values of potential vorticity are evaluated on isentropic surfaces, using the formula

$$P = -g (\zeta + f) \frac{\partial \theta}{\partial p},$$

with gravity $g = 9.8 \text{ ms}^{-2}$, Coriolis parameter f , pressure p , potential temperature θ , and relative vorticity ζ .

Table 1 gives a summary of calculated values of potential vorticity for three isentropic levels at

points where the backscatter ratio decreased to 70 %, 50 %, and 30 %, respectively. The 50 % values roughly describe the centre of maximum decrease of the backscatter ratio. A comparison of the PV values calculated at the position where the backscatter ratio decreased to 50 % with results of other investigations using PV values to describe the edge of the polar vortex are used to review our results. It should be noted that the spatial distance of the location where the backscatter ratio decreased to 70 % and 30 % in general does not differ dramatically from the position where it is reduced to 50 %. The examples given here show predominately strong gradients of the backscatter ratio.

Rummukainen et al. (1994) calculated PV at places of maximum wind speed to determine the vortex edge. For January 1993, they found a mean value of PV of $33.6 \pm 1.4 \cdot 10^{-6} \text{ K m}^2 \text{ kg}^{-1} \text{ s}^{-1}$ for the 475 K level and $77.6 \pm 2.2 \cdot 10^{-6} \text{ K m}^2 \text{ kg}^{-1} \text{ s}^{-1}$ for the 550 K level. For March 1993, they calculated a mean

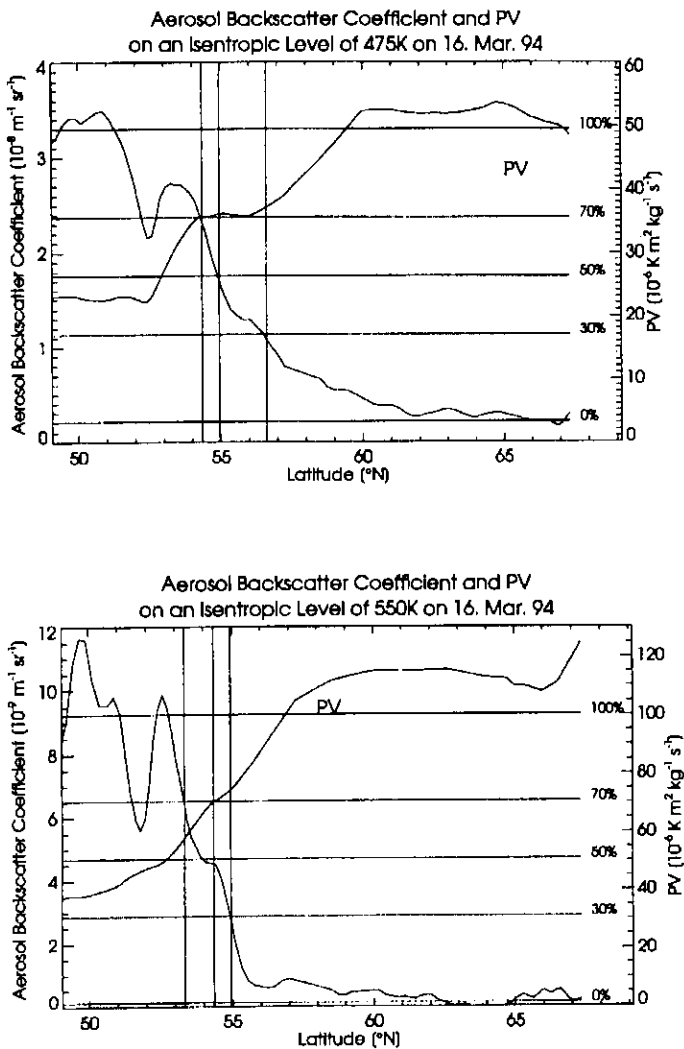


Figure 5 As Figure 2, but on 16. March 1994.

value of PV of $33.7 \pm 1.4 \cdot 10^{-6} \text{ K m}^2 \text{ kg}^{-1} \text{ s}^{-1}$ for the 475 K level and $65.4 \pm 3.0 \cdot 10^{-6} \text{ K m}^2 \text{ kg}^{-1} \text{ s}^{-1}$ for the 550 K level. Considering the limitations of such a comparison (comparison of results of single days with monthly mean values) these values agree well with the PV values calculated with respect to the aerosol measurements (cf. Table 1) for January 27 and March 10, 1993. Rummukainen and coworkers mentioned that the calculated PV values near the edge of the polar vortex remained at a relatively constant level from January to March 1993.

Manney et al. (1994a) calculated vertical sections of scaled PV for the days in late February and early March 1993. They found that the vortex edge might be reasonably defined as being near a scaled PV of $1.4 \cdot 10^{-4} \text{ s}^{-1}$ through the lower and middle stratosphere during that period. This scaled PV value was also used in the work published by Manney et al. (1994c) to describe the boundary of the polar vortex

of winter 1992/93. The scaled PV is calculated using the formula

$$\tilde{P} = \frac{P}{g \left| \frac{\partial \theta_0}{\partial p} \right|}$$

where the static stability $\frac{\partial \theta_0}{\partial p}$ is based on values of the U.S. standard atmosphere (1976). (For example, values at 475 K and 550 K are -2.1 K hPa^{-1} and -4.4 K hPa^{-1} , respectively.) $\frac{\partial \theta_0}{\partial p}$ is constant on a θ -surface (see also Dunkerton and Delisi, 1986).

An estimation of \tilde{P} based on the measured aerosol data and the related PV values for January 27 and March 10, 1993 yield a scaled PV of approximately $1.5 \cdot 10^{-4} \text{ s}^{-1}$ which is consistent with the value determined by Manney and coworkers for that period. The value of $\tilde{P} = 1.5 \cdot 10^{-4} \text{ s}^{-1}$ corresponds to $P = 21.0 \cdot 10^{-6} \text{ K m}^2 \text{ kg}^{-1} \text{ s}^{-1}$ for the 435 K, $P = 30.9 \cdot 10^{-6} \text{ K m}^2 \text{ kg}^{-1} \text{ s}^{-1}$ for the 475 K, and $P = 64.7 \cdot 10^{-6} \text{ K m}^2 \text{ kg}^{-1} \text{ s}^{-1}$ for the 550 K isentropic surface, respectively. These values are in fair agreement with the values listed in Table 1 for the measurement periods in 1993. A comparison with PV values for 1994 listed in Table 1 suggests the strength of variability from year to year and during one winter.

Figure 6 shows a three-dimensional view of the polar vortex for January 27, 1993, prescribed by the $1.5 \cdot 10^{-4} \text{ s}^{-1}$ contour of \tilde{P} . The vertical coordinate is θ , with $350 \text{ K} \leq \theta \leq 700 \text{ K}$ (approx. 10 to 30 km height). Displaying the polar vortex as a whole helps to recognize the complex structures of its boundary, for instance the grooved structures and dissociated structures. The bottom of the vortex near the tropopause indicates a plug-like appearance. It seems that the features of the boundary of the polar vortex in Figure 6 are realistic because analyses of data (PV) before and after January 27 indicate continuity in time.

4 Conclusion

LIDAR-aerosol data measured during long range missions with the German research aircraft TRANSALL have been presented. All flights directly crossed the vortex edge. The data show predominantly strong gradients of the backscatter ratio indicating a barrier to transport (mixing) and thus allowing a determination of the edge of the

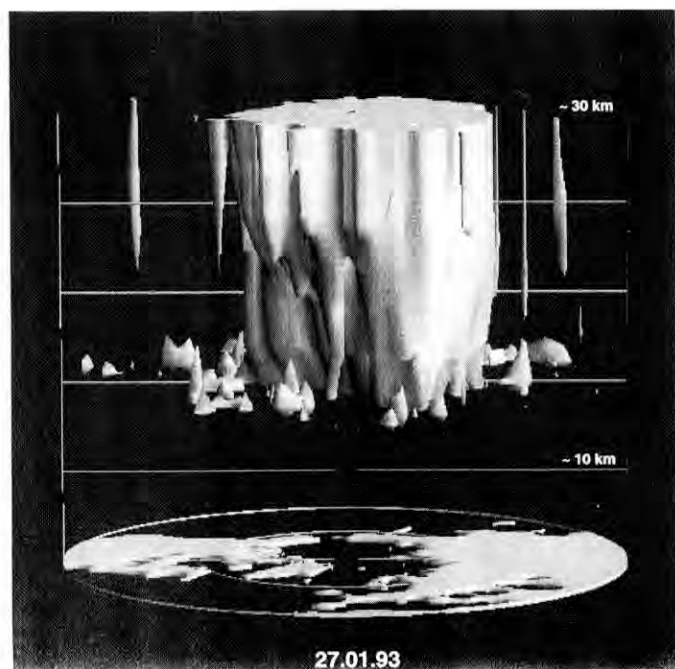


Figure 6 Three-dimensional presentation of the stratospheric polar vortex for 27 January 1993. The vortex edge is prescribed by the $1.5 \times 10^{-4} \text{ s}^{-1}$ contour of P . Latitude circles are shown at 30° and 60° N , the continents are indicated. The vertical coordinate is potential temperature θ with $350 \text{ K} \leq \theta \leq 700 \text{ K}$, approximately 10 to 30 km height.

polar vortex. The so defined vortex edge is associated with potential vorticity values which agree with those derived in previous studies as describing the location of the edge. Therefore, aerosol measurements can be used as an additional parameter to describe the structure of the vortex and especially of the vortex edge.

An advantage of high resolution aerosol measurements as presented in this paper (horizontal resolution of approximately 25 km, vertical resolution of approximately 60 m) is that they clearly resolve fine structures of the vortex edge and the surrounded area. Figure 1b additionally shows a clear example indicating the necessity of high resolution measurements to account for fine structures. It also indicates the good agreement of contours of aerosol backscatter ratio and PV, considering that the meteorological data used for the calculation of PV have a significant lower resolution ($2.5^\circ \times 2.5^\circ$). Future use of similar aerosol data would help to validate high resolution models (contour advection studies, e.g. Waugh and Plumb, 1994; Chen et al., 1994) which allow the modelling of small scale features on isentropic surfaces. This would improve the understanding of exchange and mixing processes in the vicinity of the edge of the polar vortex.

Acknowledgement

We thank two anonymous reviewers for helpful comments. This study was supported by the Bundesministerium für Forschung und Technologie, Bonn, under grants 01 LO 9215 and 01 VOZ31A/01 LO 9222. We thank ECMWF and NILU for providing the meteorological analyses.

References

- Chen, P., 1994: The permeability of the Antarctic vortex edge, *J. Geophys. Res.* **99**, 20563–20571.
- Chen, P., J. R. Holton, A. O'Neill and R. Swinbank, 1994: Quasi-horizontal transport and mixing in the Antarctic stratosphere, *J. Geophys. Res.* **99**, 16851–16866.
- Deshler, T., 1994: In situ measurements of Pinatubo aerosol over Kiruna on four days between 18 January and 13 February 1992, *Geophys. Res. Lett.* **21**, 1323–1326.
- Dunkerton, T. J. and D. P. Delisi, 1986: Evolution of potential vorticity in the winter stratosphere of January–February 1979, *J. Geophys. Res.* **91**, 1199–1208.
- Günther, G. and M. Dameris, 1995: Air mass exchange across the polar vortex edge during a simulated major stratospheric warming, *Ann. Geophysicae*, in press.
- Manney, G. L. and R. W. Zurek, 1993: Interhemispheric comparison of the development of the stratospheric polar vortex during fall: A 3-dimensional perspective for 1991–1992, *Geophys. Res. Lett.* **20**, 1275–1278.
- Manney, G. L., L. Froidevaux, J. W. Waters, R. W. Zurek, W. G. Read, L. S. Elson, J. B. Kumer, J. L. Mergenthaler, A. E. Roche, A. O'Neill, R. S. Harwood, I. MacKenzie and R. Swinbank, 1994a: Chemical depletion of ozone in the Arctic lower stratosphere during winter 1992–93, *Nature* **370**, 429–434.
- Manney, G. L., R. W. Zurek, A. O'Neill and R. Swinbank, 1994b: On the motion of air through the stratospheric polar vortex, *J. Atmos. Sci.* **51**, 2973–2994.
- Manney, G. L., R. W. Zurek, M. E. Gelman, A. J. Miller and R. Nagatani, 1994c: The anomalous arctic lower stratospheric polar vortex of 1992–1993, *Geophys. Res. Lett.* **21**, 2405–2408.
- McIntyre, M. E. and T. N. Palmer, 1983: Breaking planetary waves in the stratosphere, *Nature* **305**, 593–600.
- Randel, W., 1993: Ideas flow on antarctic vortex, *Nature* **364**, 105–106.
- Rummukainen, M., B. Knudsen, P. von der Gathen, 1994: Dynamical diagnostics of the edges of the polar vortices, *Ann. Geophysicae* **12**, 1114–1118.
- U. S. Standard Atmosphere, 1976: U. S. government printing office, Washington D.C.
- Waugh, D. W. and R. A. Plumb, 1994: Contour advection with surgery: A technique for investigating finescale structure in tracer transport, *J. Atmos. Sci.* **51**, 530–540.
- Waugh, D. W., R. A. Plumb, R. J. Atkinson, M. R. Schoeberl, L. R. Lait, P. A. Newman, M. Loewenstein, D. W. Toohey, L. M. Avallone, C. R. Webster and R. D. May, 1994: Transport out of the lower stratospheric Arctic vortex by Rossby wave breaking, *J. Geophys. Res.* **99**, 1071–1088.
- Wirth, M., G. Ehret, P. Mörl and W. Renger, 1994: Two dimensional stratospheric aerosol distribution during EASOE, *Geophys. Res. Lett.* **21**, 1287–1290.